August, 2006

High-resolution real-time 3D absolute coordinates measurement using a fast three-step phase-shifting algorithm

Song Zhang, *Harvard University*
Dale Royer
Shing-Tung Yau, *Harvard University*

High-Resolution, Real-Time 3-D Absolute Coordinates Measurement Using a Fast Three-Step Phase-Shifting Algorithm

Song Zhang[a], Dale Royer[b] and Shing-Tung Yau[a]
[a] Department of Mathematics, Harvard University, Cambridge, MA 02138
[b] Geometric Informatics Inc, Somerville, MA 02143
Email: szhang@fas.harvard.edu, dale.royer@geometricinformatics.com, yau@math.harvard.edu

ABSTRACT

High-resolution, real-time 3-D absolute coordinate measurement is highly important in many fields. This paper presents such a system that measures 3-D absolute geometric shapes and positions at 30 frames per second (fps), with an image resolution of 532×500. The system is based on a digital fringe projection and fast three-step phase-shifting method. It utilizes a digital-light-processing (DLP) projector to project color encoded computer generated phase-shifted fringe patterns in grayscale, a high-speed CCD camera synchronized with the projector to capture fringe images at 90 fps. Based on the three-step phase-shifting algorithm, any successive three fringe images can be used to reconstruct one 3-D shape. Therefore, the 3-D shape measurement speed is 30 fps. To obtain absolute coordinates, absolute phase is required. In this research, a tiny marker is encoded in the projected fringe pattern, and detected by software from captured fringe images accurately. Absolute coordinates can be obtained when the marker position is located and the measurement system is calibrated. To demonstrate the performance of the system, we measured human faces. The details of facial geometries and dynamic changes of facial expressions are measured clearly. We also measured a hand moving over a depth distance of approximately 700mm, again both hand shapes and positions changes are clearly captured. By using the fast three-step phase-shifting algorithm and a parallel processing technique, we successfully developed a system that acquires, reconstructs, and displays 3-D shape in real-time. Applications of such a system include manufacturing, inspection, reverse engineering, computer vision and computer graphics.

Keywords: High resolution, real time, absolute coordinates, 3-D shape measurement, phase shifting, digital fringe projection

1. INTRODUCTION

Accurate real-time 3-D geometric shape measurement is increasingly important, with applications in manufacturing, inspection, human computer interactions, virtual reality, geometric modelling, entertainment, plastic surgery, homeland security, etc.

Optical 3-D ranging methods,[1] including stereovision, laser triangulation, and structured light, are extensively employed due to its non-contact and non-destructive nature. Among all existing ranging techniques, stereovision is probably the most studied method.[2] However, the shortcoming of a stereo-based method is that the matching of stereo images is usually time-consuming. It is therefore difficult to realize real-time 3-D shape reconstruction from stereo images. With the development of digital video display technologies, the structured-light-based techniques are becoming more and more widely used. A structured light system differs from a stereo system by replacing one of cameras of the stereo system with a projector. The projector projects certain coded structured patterns to help registration. Unlike stereo-based methods, structured-light-based methods usually use processing algorithms that are much simpler. Therefore, it is more likely for them to achieve real-time performance.

There are essentially two approaches toward real-time 3-D shape measurement. One approach is to use a single pattern, typically a color pattern.[3–6] Because they use color to code the patterns, the shape measurement result is affected, to varying degrees, by the variations of the object surface color. Guan et al. proposed a method that uses a composite structured light pattern to realize real-time 3-D shape measurement.[7] It is an attractive approach to realize absolute coordinate measurement by using a single fringe pattern. However, the resolution achieved is not high. The other approach is to use multiple patterns while switching them rapidly so that the number of patterns required to reconstruct one 3-D

Interferometry XIII: Techniques and Analysis, edited by Katherine Creath, Joanna Schmit,
Proc. of SPIE Vol. 6292, 62920M, (2006) · 0277-786X/06/$15 · doi: 10.1117/12.677343

shape can be captured in a short period of time. Rusinkiewicz et al. developed a real-time 3-D model acquisition system that utilizes four patterns coded with stripe boundary codes.[8] The data acquisition speed achieved was 15 frames per second (fps), which is sufficient for scanning slowly moving objects. Since the system is based on a binary-coding method, the spatial resolution is relatively low because the stripe width must be larger than one pixel. Huang et al. proposed a high-speed 3-D shape measurement technique based on a rapid phase-shifting technique.[9] They use three phase-shifted, sinusoidal fringe patterns to achieve pixel-level resolution. Zhang and Huang developed a 3-D shape acquisition system that realized a 3-D shape acquisition speed of up to 40 fps.[2] It is good enough to measure dynamic shapes within a small depth range. However, the system can only measure relative geometric shape changes, namely, it cannot measure rigid motion in depth direction beyond 2π. Moreover, because of the phase-to-height conversion algorithm used, the measurement error is significant large if the object is far away from the so called "reference plane", or if the measurement depth range is comparable with the distance from the scanner.

To our knowledge, it is very difficult for any existing 3-D shape measurement system to obtain absolute coordinates in real-time with high resolution. This paper presents a revised version of the system developed by Zhang and Huang.[2] It is based on a digital fringe projection and phase-shifting method. Three phase-shifted fringe patterns, coded with three primary color channels (RGB), are sent to a DLP projector in B/W mode and captured by a high-speed CCD camera synchronized with the projector. The data acquisition speed is 90 fps. Based on the fast three-step phase-shifting algorithm used in this research, any successive three images can be used to reconstruct one 3-D shape, therefore, the 3-D data acquisition speed is 30 fps. This system can measure absolute coordinates of the objects, that is, both geometric shapes and positions can be acquired. Since the absolute coordinates are measured, the system can significantly reduce the distortion error caused by the phase-to-height approximations as used in the system developed by Zhang and Huang.[2] Therefore, the measurement depth range can be significantly larger, 700 mm for our system. The absolute coordinates measurement is possible only when absolute phase can be obtained. In order to obtain absolute phase, Hu et al.[10] and Zhang and Huang[11] used an additional centerline image. However, it is not desired for this research since our research focus is to develop a high-speed 3-D shape system, while increasing the number of fringe images to reconstruct one 3-D shape will decrease the measurement speed. In this research, a tiny cross marker is encoded in the projected fringe images, so that the 3-D data acquisition speed is maintained but the absolute phase can be obtained. We propose a marker detection algorithm that takes advantage of epipolar geometry, one point from the projector is imaged to one line on the camera image. It utilizes the information from both the 2-D texture image and the gamma map. Our experiments demonstrate that more than 99% markers can be correctly detected using the proposed method. In order to boost the robustness of the marker detection algorithm, a marker tracking algorithm is developed. This algorithm tune the incorrectly detected marker points to the right position by checking that of the neighboring frames. The absolute coordinates can be calculated from absolute phase if the system is calibrated.

Section 2 explains the principle. Section 3 shows experimental results. Section 4 concludes the paper.

2. PRINCIPLE

2.1. Fast three-step phase-shifting algorithm

Phase-shifting methods are extensively employed in optical metrology, especially with the development of digital computers and digital display technologies. Three-step phase-shifting algorithms have the advantage of fast measurement because they require the minimum number of fringe images to reconstruct one 3-D shape.[12] In this research, the fast three-step phase-shifting algorithm proposed by Huang and Zhang is used.[13] The intensities of the fringe images can be written as,

$$\begin{aligned} I_1(x,y) &= I'(x,y) + I''(x,y)\cos[\phi(x,y) - 2\pi/3], && (1)\\ I_2(x,y) &= I'(x,y) + I''(x,y)\cos[\phi(x,y)], && (2)\\ I_3(x,y) &= I'(x,y) + I''(x,y)\cos[\phi(x,y) + 2\pi/3], && (3)\end{aligned}$$

where $I'(x,y)$ is the average intensity, $I''(x,y)$ the intensity modulation, and $\phi(x,y)$ the phase.

Instead of solving phase using an arctangent function, the fast three-step phase-shifting algorithm approximates the phase by

$$\phi(x,y) = \frac{\pi}{3}\left[2 \times \text{round}\left(\frac{N}{2}\right) + (-1)^N r(x,y)\right] \tag{4}$$

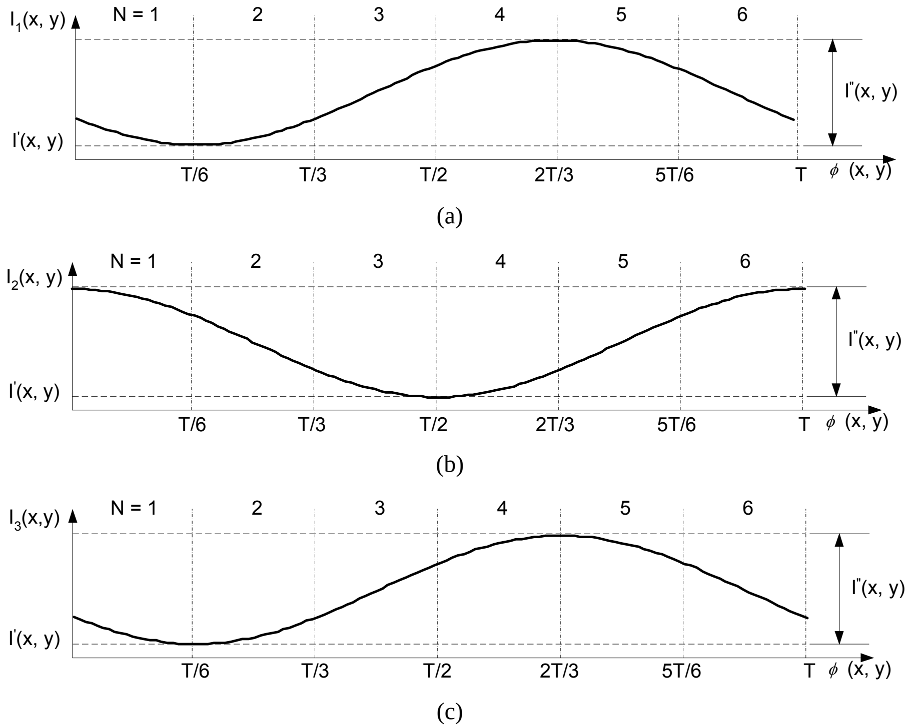

Figure 1. Cross sections of the three phase-shifted sinusoidal fringe patterns. (a) $I_1(-2\pi/3)$. (b) $I_2(0)$. (c) $I_3(2\pi/3)$

with

$$r(x,y) = \frac{I_{med}(x,y) - I_{min}(x,y)}{I_{max}(x,y) - I_{min}(x,y)}\,, \tag{5}$$

where $r(x,y)$ is the so called intensity ratio whose value ranges from 0 to 1. $N = 1,2,...,6$ is the region number, as shown in Figure 1. One fringe period (2π) is evenly divided into six regions, each region covers an angular range of $\pi/3$. $I_{min}(x,y)$, $I_{med}(x,y)$, and $I_{max}(x,y)$ are denoted as the minimum, median, and maximum intensity values respectively. In addition, a small look-up-table (LUT) (256 elements) is utilized to reduce for the approximation error. Huang and Zhang demonstrated that after the LUT error compensation, the error of the phase approximation is approximately ± 0.0002 radians, which is negligible. However, the phase wrapping speed is 3.4 times faster than traditional method that uses an arctangent function,[13] which is critical for real-time 3-D shape reconstruction. The phase $\phi(x,y)$ obtained in Eq. (4) is the so-called modulo 2π at each pixel, whose value ranges from 0 to 2π. If the fringe patterns contain multiple fringes, phase unwrapping is necessary to remove the sawtooth-like discontinuities and obtain a continuous phase map.[14] Once the continuous phase map is obtained, the phase at each pixel can be converted to *xyz* coordinates of the corresponding point on the object surface through calibration.[10,11,15] The average intensity $I'(x,y)$ represents a flat image of the measured object and can be used for texture mapping.

Solving Eqs. (1)-(3) simultaneously, we can obtain data modulation

$$\gamma(x,y) = \frac{I''(x,y)}{I'(x,y)} = \frac{\sqrt{3(I_1 - I_3)^2 + (2I_2 - I_1 - I_3)^2}}{I_1 + I_2 + I_3}. \tag{6}$$

Data modulation $\gamma(x,y)$ has a value between 0 and 1 and can be used to determine the quality of the phase data at each pixel with 1 being the best.

2.2. Marker detection

To reduce the measurement error caused by the marker, a tiny marker is used. However, locating the tiny marker from 2-D image is difficult especially when the image is blurred. Figure 3(a) shows a typical example. The cross marker in

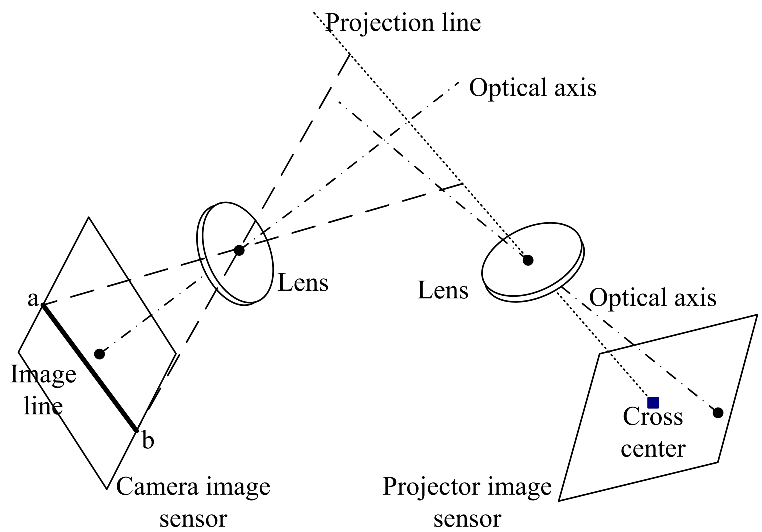

Figure 2. Schematic diagram of the epipolar geometry of a structured light system

the elliptical white window is barely visible. To detect the marker automatically, we generate a gamma map using Eq. (6), which is shown in Figure 3(b), where the marker is more clearly stood out. However, in general, detecting the marker from the gamma map is not easy. In this research, a mask is created based on the texture image and gamma map, and is used to remove the background. The gamma map is also inverted: black to be white, and vice versa. Figure 3(c) shows the inverted gamma map after implementing the mask. Even though, our experiments showed that detecting cross accurately still failed sometimes. To improve the robustness of this procedure, a constraint is found to be helpful. Figure 2 shows the schematic diagram of the structured light system. From epipolar geometry, [16] the ray of the cross center projected by the projector is imaged onto a horizontal line *ab* in Figure 2 on the camera image if there is no camera lens distortion. And this line can be calibrated. The marker searching only needs to be performed on the calibrated line, which makes the searching faster and more robust. We use a template-based method to find the marker center. The template we use is a 5×5 array,

$$f(x,y) = \begin{bmatrix} 0 & 1 & 1 & 1 & 0 \\ 1 & 1 & 2 & 1 & 1 \\ 1 & 2 & 4 & 2 & 1 \\ 1 & 1 & 2 & 1 & 1 \\ 0 & 1 & 1 & 1 & 0 \end{bmatrix}.$$

Assume the calibrated line is $y = h(x)$ for $x \in [1, w]$, where w is image width. Functional

$$g(x,h(x)) = \sum_{i=-2}^{i=2} \sum_{j=-2}^{j=2} \left\{ [w_g \times I_g(x+i, h(x)+j) + w_t \times I_t(x+i, h(x)+j)] \, f(i+2, j+2) \right\} \tag{7}$$

is defined to find the marker center. The center is located at the point where $g(x,h(x))$ reaches the maximum. Here, I_g is the inverted gamma map, I_t is the texture image, w_g is the weight for the gamma map, and w_t is the weight for the texture image. We consider both the texture and the gamma map to minimize the effect of noise and background. Our experiments show that more than 99% markers can be correctly detected using this method.

2.3. Marker tracking

To further improve the marker detection accuracy, we developed an marker tracking algorithm. Since the frame rate is very high, we can assume the marker moves slowly from frame to frame. The marker positions over time form a vector field,

$$\vec{v}_i := p(t_i) - p(t_{i-1}). \tag{8}$$

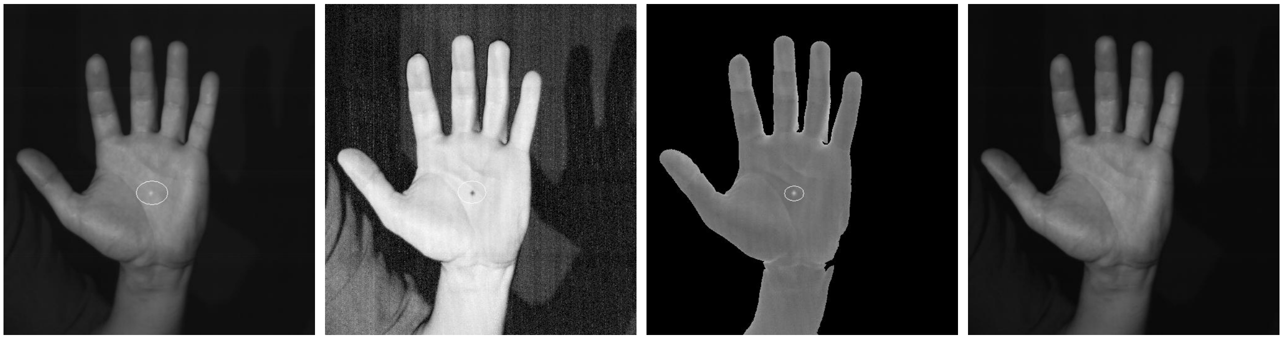

Figure 3. Marker detection and removal. (a) 2-D texture image with the marker. (b) Gamma map of the fringe images. (c) Inverted gamma map of the fringe images. (d) Texture image after the maker is removed.

The length of the vector $\vec{v}_i$, $||\vec{v}_i||$, can be used to determine whether $p(t_i)$ or $p(t_{i-1})$ is incorrectly identified. Figure 4 shows a typical case of $||\vec{v}_i||$ for a sequence of 300 frames. Cross movements of most frames are very small. If the value is larger than a pre-selected threshold v_{th} (green dashed line), frame t_i is marked as an incorrect frame. Figure 4(a) marked incorrect frames with a blue centered red box. The longest interval without any incorrect frames is regarded as the longest good segment (between frames 100 and 250), and all marker positions in that segment are regarded as correctly found. Assume the good segment starts at t_{start} frame and ends at t_{end} frame, as magenta points shown in Figure 4(b).

Once the good segment is determined, the "bad" and "good" frames can be identified. if the average moving speed of the cross is $\vec{v}_{avg} := \sum_{i=start}^{i=end} \vec{v}_i/(t_{start} - t_{end} + 1)$. "Good" and "bad" frames on the right side of the longest good segment can be marked by the following steps:

1. Start with a good frame t_s, whose cross position is $p(t_s)$.
2. **for** $j \leftarrow s+1$ **to** *end*
   Go right to frame t_j
   if $||p(t_j) - p(t_s)|| > ||v_{th}|| + ||(t_j - t_s)\vec{v}_{avg}||$
       frame t_j is regarded as bad
   else
       frame t_j is regarded as good, $t_s \leftarrow t_j$
   loop.

Similarly, "bad" and "good" frames can be marked on the left hand side. Red points and blue points in Figure 4(b) are detected "bad" frames and "good" frames respectively.

Once "good"(magenta and blue in Figure 4(b)) and "bad" (red in Figure 4(b)) frames are determined, spline functions can be used to fit cross movement over time $x(t)$ and $y(t)$ using good frames. Cross positions for bad frames can be calculated from these spline functions.

2.4. Absolute phase to coordinate conversion

Once the marker is detected, absolute phase can be obtained by shifting the whole phase map to make the marker point phase, ϕ_0, to be absolute zero,

$$\phi_a(x,y) = \phi(x,y) - \phi_0(x_0,y_0). \tag{9}$$

Each point on the camera captured fringe image corresponds to one line with the same absolute phase on the projected fringe image.[11] Therefore, a relationship between the captured fringe image and the projected fringe image can be established,

$$\phi_a(u_c,v_c) = \phi_a(u_p). \tag{10}$$

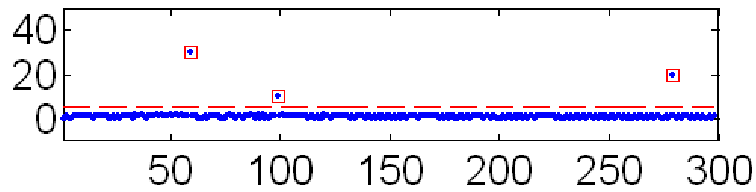

(a)

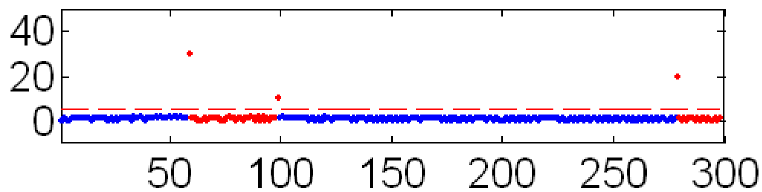

(b)

Figure 4. Marker detection and tracking. (a) Cross moving distance from frame to frame. (b) Detection of fake cross positions.

In this research, the structured light system is calibrated by using the method proposed by Zhang and Huang.[11,17] This method is essentially to allow the projector to capture images like a camera. The projector can be calibrated independently and quickly follows the calibration procedure of the camera. Therefore, the structured light system calibration becomes a well-studied stereo system calibration. It is an elegant structured light system calibration method that significantly simplifies the system calibration procedure. After calibration, the intrinsic parameters matrices for the camera A_c and the projector A_p can be obtained. The extrinsic parameter matrices, in a fixed world coordinate system, for the camera M_c and the projector M_p are obtained. Once the system is calibrated, the relationships between the world coordinate system and the camera coordinate system and between the world coordinate system and the projector coordinate system can be established,

$$s_c[u_c, v_c, 1]^T = A_c M_c [X_w, Y_w, Z_w, 1]^T, \tag{11}$$
$$s_p[u_p, v_p, 1]^T = A_p M_p [X_w, Y_w, Z_w, 1]^T \tag{12}$$

s_c, s_p are the camera and the projector scaling factor, respectively, (u_c, v_c) and (u_p, v_p) are the camera and the projector image coordinates, respectively, and (X_w, Y_w, Z_w) is the world coordinates.

In Eqs. (10)-(12), (X_w, Y_w, Z_w), s_c, s_p u_p, and v_p are the seven unknowns, since there are seven independent equations, the world coordinate (X_w, Y_w, Z_w) can be uniquely determined.

2.5. Marker removal

The marker on the 2-D flat images needs to be removed if hight quality texture image is required. However, it is difficult to remove the marker without artifacts from the texture image. Figure 3(a) shows a typical example before the marker is removed. In this research, a method is found to be able to remove the markers completely without any artifacts.

Ideally, if no noises exists, from the properties of the fast three-step phase shifting algorithm, the data modulation ($\gamma(x,y)$ in Eq. (6)) should be always 1 across the image with coded fringe patterns. In the meantime, the intensity value on "cross" marker pixels is I_0 for all three images, namely, $I_1 = I_2 = I_3 = I_0$. Therefore, Eq. (6), $\gamma = 0$ for points on the marker. Since the three fringe images with a phase shift of 120°, the 2-D texture images can be obtained by averaging three fringe images,

$$t(x,y) = \begin{cases} (I_1 + I_2 + I_3)/3 = I' & (x,y) \in \text{fringe area} \\ I_0 & (x,y) \in \text{marker area} \end{cases}. \tag{13}$$

We define a functional,

$$f(x,y) = (I_1 + I_2 + I_3)/3(1+\gamma(x,y))/2 \tag{14}$$

$$= \begin{cases} I'(x,y) & (x,y) \in \text{fringe area} \\ I_0/2 & (x,y) \in \text{marker area} \end{cases} \tag{15}$$

if $I_0 = 2I'$, functional $f(x,y)$ is the same across image, hence the marker is cleanly removed. Assume the intensities of projected fringe images generated by the computer are,

$$I_1(x,y) = a + b(1+\cos(\phi(x,y) - 2\pi/3)), \tag{16}$$

$$I_2(x,y) = a + b(1+\cos(\phi(x,y))), \tag{17}$$

$$I_3(x,y) = a + b(1+\cos(\phi(x,y) + 2\pi/3)). \tag{18}$$

It is clear that if $a + b = I_c$, the markers can be guaranteed to be cleanly removed. Here I_c is the intensity value for the markers, which is 255 in our case.

Figure 3(d) shows that the result after removing the marker shown in Figure 3(a). It is clearly shows that the marker is cleanly removed.

3. EXPERIMENTS

To verify the performance of the real-time system, we measured a human face. Figure 5 shows one measurement result of a heavily beard male face. First row from left to right: phase shifted fringe images $I_1(-2\pi/3)$, $I_2(0)$ and $I_3(2\pi/3)$, the wrapped phase map with phase values ranges from 0 to 2π. The second row from left to right, the mask map with white to be good pixels, the unwrapped phase map, the texture image with the detected marker point denoted as a red dot, and the 3-D geometry. The 3-D measurement result clearly demonstrate that our system can measure absolute 3-D geometry satisfactorily. We then measured a human face with expressions. The 3-D data is acquired at 30 fps. Figure 6 shows six selected frames from a sequence of 100 frames. During the experiment, the subject was asked to smile so that facial expressions are introduced. The process of a smile is clearly captured, and the facial geometries details are acquired accurately. This experiment shows the feasibility of measuring geometric facial expressions.

In addition, to test the robustness of the marker detection and tracking algorithm, we measured a hand moving slowly over a distance of approximately 700 mm. A total number of 300 frames was acquired. Figure 7 shows two extreme cases: the nearest most and the far most. The first frame as shown in Figure 7 first row shows the closest frame with the bright fringe images and clear cross markers. The texture is clear and bright and the cross marker can be clearly seen. Figure 7 second row shows the farthest frame with the fringe images darker and blurred. The cross marker is barely visible. Figure 7 first column shows one of the fringe images, while Figure 7 second column shows the texture image by averaging three phase-shifted fringe images. Figure 7 third column shows the detected cross marker center as red dot. The 3-D geometry is shown in Figure 7 fourth column. This experiments shows that the system can capture *absolute* coordinates of the object, namely, it can measure both geometric shapes and positions. It also shows that the feature details are clearly captured once the object is in focus and the fringe images are bright, while noisier when the object is far away from focal plane, e.g., when the fringe images are defocused and dark. This is because when the fringe images are darker, the signal-to-noise is smaller. This experiment also demonstrate that our system can measure both geometric shapes and positions for a relatively large depth range. More data and videos are available at http://math.harvard.edu/˜songzhang

4. CONCLUSION AND FUTURE WORK

This paper presents a high-resolution, real-time 3-D absolute coordinates measurement system based on fast three-step phase-shifting method. The data acquisition speed is 30 fps with 266K points per frame. Absolute 3-D coordinates are obtained from three fringe images with a tiny marker. We propose a marker detection and tracking algorithm that takes advantage of epipolar geometry, one point from the projector is imaged to one line on the camera image. It utilizes the information from both the 2-D texture image and the gamma map. Our experiments demonstrate that more than 99% markers can be correctly detected using the proposed method. Absolute coordinate is computed with the detected marker and the calibrated system. We successfully demonstrate that our system can capture the details of facial expressions, both

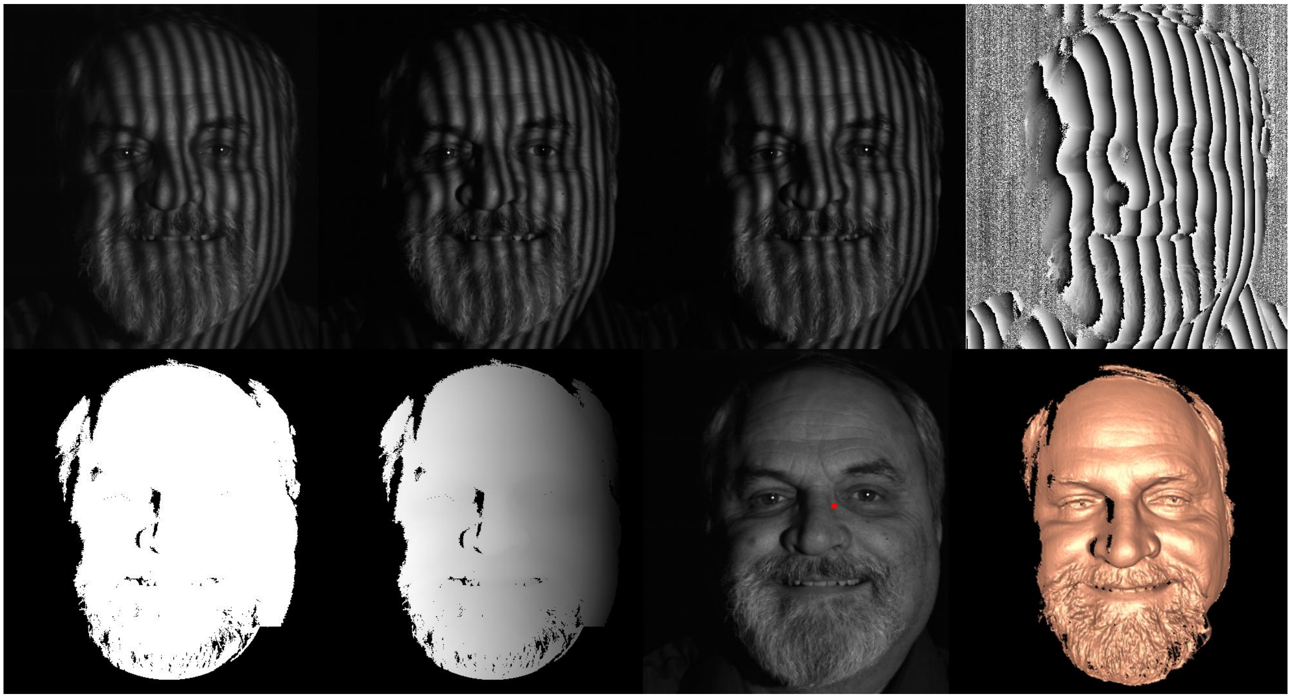

Figure 5. Measurement results of a human face. First row from left to right: phase shifted fringe images $I_1(-2\pi/3)$, $I_2(0)$ and $I_3(2\pi/3)$, the wrapped phase map with phase values ranges from 0 to 2π. The second row from left to right, the mask map with white to be good pixels, the unwrapped phase map, the texture image with the detected marker point denoted as a red dot, and the 3-D geometry.

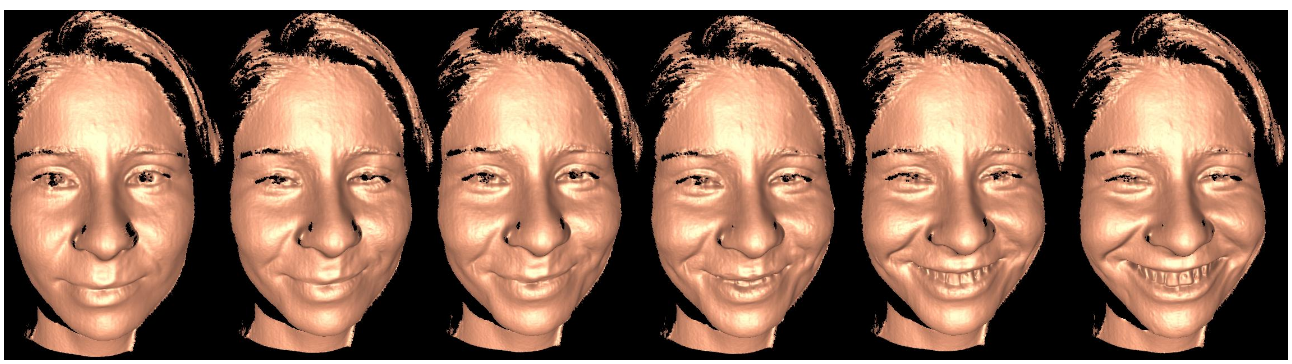

Figure 6. Measurement result of human expressions. Six frames selected from a smiling sequence of 100 of a subject. The 3-D data acquisition speed is 30 fps.

geometric shapes and positions of the hand moving over a depth range of 700 mm. To obtain high-quality texture images, we propose a method that can remove the marker cleanly. Although not relevant to metrology, it is important in applications such as computer graphics and computer vision.

In the system described in Refs.,[17,18] real-time 3-D relative geometry acquisition, reconstruction, and display was successfully realized. However, the current system takes approximately 0.2 sec to compute absolute coordinates of one geometric shape with a Dell Precision 670 workstation (Pentium 4 3.4GHz). To realize real-time 3-D absolute coordinate measurement, the computational efficiency of the marker detection and the absolute phase-to-coordinate conversion algorithms has to be improved.

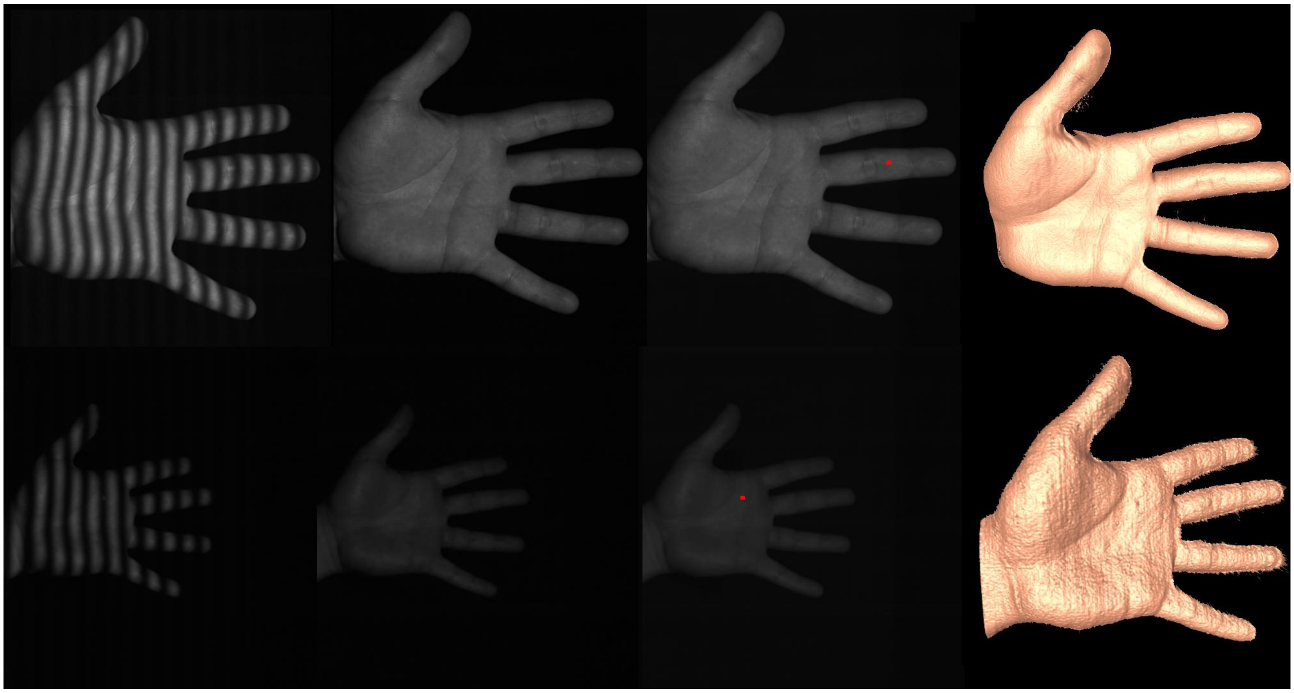

Figure 7. Result of marker detection and tracking algorithm. A hand moving continuously over a depth distance of 700 mm is measured, 300 frames are captured. The first row shows the nearest frame, and the second row shows the farthest frame.

Acknowledgment

We want to thank Gene Royer, Vicki Royer, Franciane Royer, Mark Royer, Anna Royer, Lori Royer, and Jeffrey Shattuck for serving as models. This work was done at Geometric Informatics Inc funded by the Advanced Technology Program (ATP) of the National Institute of Standards and Technology (NIST).

REFERENCES

1. J. Salvi, J. Pages, and J. Batlle, "Pattern codification strategies in structured light systems," *Pattern Recogn.* **37**(4), pp. 827–849, 2004.
2. S. Zhang and P. Huang, "High-resolution, real-time 3-d shape acquisition," in *IEEE Computer Vision and Pattern Recognition Workshop on Real-time 3D Sensors and Their Uses*, **3**, pp. 28–37, 2004.
3. K. G. Harding, "Phase grating use for slop discrimination in moiré contouring," in *Proc. SPIE, Optics, illumination, and image sensing for machine vision VI* **1614**, pp. 265–270, 1991.
4. Z. J. Geng, "Rainbow 3-d camera: New concept of high-speed three vision system," *Opt. Eng.* **35**, pp. 376–383, 1996.
5. C. Wust and D. W. Capson, "Surface profile measurement using color fringe projection," *Machine Vision and Applications* **4**, pp. 193–203, 1991.
6. P. S. Huang, Q. Hu, F. Jin, and F. P. Chiang, "Color-encoded digital fringe projection technique for high-speed three-dimensional surface contouring," *Opt. Eng.* **38**, pp. 1065–1071, 1999.
7. C. Guan, L. G. Hassebrook, and D. L. Lau, "Composite structured light pattern for three-dimensional video," *Opt. Express* **11**, pp. 406–417, 2003.
8. S. Rusinkiewicz, O. Hall-Holt, and L. Marc, "Real-time 3d model acquisition," in *SIGGRAPH*, pp. 438 – 446, 2002.
9. P. S. Huang, C. Zhang, and F. P. Chiang, "High-speed 3-d shape measurement based on digital fringe projection," *Opt. Eng.* **42**(1), pp. 163–168, 2003.
10. Q. Hu, P. S. Huang, Q. Fu, , and F. P. Chiang, "Calibration of a 3-d shape measurement system," *Opt. Eng.* **42**, pp. 487–493, 2003.
11. S. Zhang and P. S. Huang, "A novel structured light system calibration," *Opt. Eng.* , 2006. In Press.

12. D. Malacara, ed., *Optical Shop Testing*, John Wiley and Songs, NY, 1992.
13. P. S. Huang and S. Zhang, “A fast three-step phase shifting algorithm,” *Appl. Opt.* , 2006. In Press.
14. D. C. Ghiglia and M. D. Pritt, *Two-Dimensional Phase Unwrapping: Theory, Algorithms, and Software*, John Wiley and Sons, Inc, 1998.
15. R. Legarda-Sáenz, T. Bothe, and W. P. Jüptner, “Accurate procedure for the calibration of a structured light system,” *Opt. Eng.* **43**, pp. 464–471, 2004.
16. D. A. Forsyth and J. Ponce, *Computer Visoin- A Modern Approach (Chapter 3)*, Prentice-Hall, Inc., New Jersey, 2002.
17. S. Zhang, *High-resolution, Real-time 3-D Shape Measurement*. PhD thesis, Stony Brook University, Stony Brook, New York, 2005.
18. S. Zhang and P. S. Huang, “High-resolution, real-time 3-d shape measurement,” *Opt. Eng.* , 2006. In Press.